BIOMIMETIC MULTI-CHANNEL MICROSTIMULATION OF SOMATOSENSORY CORTEX CONVEYS HIGH RESOLUTION FORCE FEEDBACK FOR BIONIC HANDS

Charles M. Greenspon[1], Giacomo Valle[1], Taylor G. Hobbs[2], Ceci Verbaarschot[2,3], Thierri Callier[4], Natalya D. Shelchkova[4], Anton R. Sobinov[1], Patrick M. Jordan[1], Jeffrey M. Weiss[2], Emily E. Fitzgerald[1], Dillan Prasad[1], Ashley van Driesche[1], Ray C. Lee[5], David Satzer[6], Jorge Gonzalez-Martinez[7], Peter C. Warnke[6], Lee E. Miller[8,9,10,11], Michael L. Boninger[2,3,12], Jennifer L. Collinger[2,3,12,13], Robert A. Gaunt[2,3,12,13], John E. Downey[1], Nicholas G. Hatsopoulos[1,3,14], Sliman J. Bensmaia[1,3,14, ¥]

[1] Department of Organismal Biology and Anatomy, University of Chicago, Chicago, IL
[2] Rehab Neural Engineering Labs, University of Pittsburgh, Pittsburgh, PA
[3] Department of Physical Medicine and Rehabilitation, University of Pittsburgh, Pittsburgh, PA
[4] Committee on Computational Neuroscience, University of Chicago, Chicago, IL
[5] Schwab Rehabilitation Hospital, Chicago, IL
[6] Department of Neurological Surgery, University of Chicago, Chicago, IL
[7] Department of Neurosurgery, University of Pittsburgh, Pittsburgh, PA
[8] Department of Neuroscience, Northwestern University, Chicago, IL
[9] Department of Biomedical Engineering, Northwestern University, Evanston, IL
[10] Department of Physical Medicine and Rehabilitation, Northwestern University, Chicago, IL
[11] Shirley Ryan Ability Lab, Chicago, IL
[12] Department of Bioengineering, University of Pittsburgh, Pittsburgh, PA
[13] Department of Biomedical Engineering, Carnegie Mellon University, Pittsburgh, PA
[14] Neuroscience Institute, University of Chicago, Chicago, IL

[¥]For correspondence: sliman@uchicago.edu

ACKNOWLEDGMENTS

We would like to thank the participants for their generous contribution to the advancement of science. This work was supported by NINDS grants UH3 NS107714 and R35 NS122333.

DISCLOSURES

NH and RG serve as consultants for Blackrock Neurotech, Inc. RG is also on the scientific advisory boards of Braingrade GmbH and Neurowired LLC. MB, JC, and RG receive research funding from Blackrock Neurotech, Inc. though that funding did not support the work presented here.

ABSTRACT

Manual interactions with objects are supported by tactile signals from the hand. This tactile feedback can be restored in brain-controlled bionic hands via intracortical microstimulation (ICMS) of somatosensory cortex (S1). In ICMS-based tactile feedback, contact force can be signaled by modulating the stimulation intensity based on the output of force sensors on the bionic hand, which in turn modulates the perceived magnitude of the sensation. In the present study, we gauged the dynamic range and precision of ICMS-based force feedback in three human participants implanted with arrays of microelectrodes in S1. To this end, we measured the increases in sensation magnitude resulting from increases in ICMS amplitude and participant's ability to distinguish between different intensity levels. We then assessed whether we could improve the fidelity of this feedback by implementing "biomimetic" ICMS-trains, designed to evoke patterns of neuronal activity that more closely mimic those in natural touch, and by delivering ICMS through multiple channels at once. We found that multi-channel biomimetic ICMS gives rise to stronger and more distinguishable sensations than does its single-channel counterpart. We conclude that multi-channel biomimetic ICMS conveys finely graded force feedback that more closely approximates the sensitivity conferred by natural touch.

INTRODUCTION

Manual interactions with objects rely critically on tactile signals from the hand, as evidenced by the deficits incurred when these signals are lost or eliminated *(1–3)*. With this in mind, efforts are under way to provide brain-controlled bionic hands with tactile feedback via intracortical microstimulation (ICMS) of somatosensory cortex (S1)*(4, 5)*, which has been shown to evoke vivid tactile percepts *(6, 7)* and improve control of prosthetic hands *(8)*. To be useful, tactile feedback needs to convey information about contact events, including information about contact location and force. Information about location can be intuitively conveyed by matching force sensors on the bionic hand with somatotopically appropriate electrodes in S1 *(6, 8, 9)*. For example, a force sensor on the index fingertip of the bionic hand drives stimulation of electrodes located in the index representation of S1, thus producing a sensation experienced on the index finger. Information about contact force can be conveyed by modulating ICMS amplitude according to the output of the sensor, where higher stimulation amplitudes give rise to more intense touch sensations, paralleling the sensory correlates of increases in force on the skin *(6, 9, 10)*.

The objective of the present study was to examine the precision and accuracy of ICMS-based tactile feedback about contact force in three human participants implanted with arrays of microelectrodes in S1. To this end, we first characterized the increases in sensation magnitude resulting from increases in ICMS amplitude (cf. ref *(6)*) and gauged the intensity of these percepts against tactile benchmarks. We found that the intensity of ICMS-evoked sensations was highly electrode dependent and often faint. Furthermore, only a few discriminable levels of intensity could be achieved using standard force feedback, which consists of linearly modulating ICMS amplitude according to the applied force. Seeking to improve

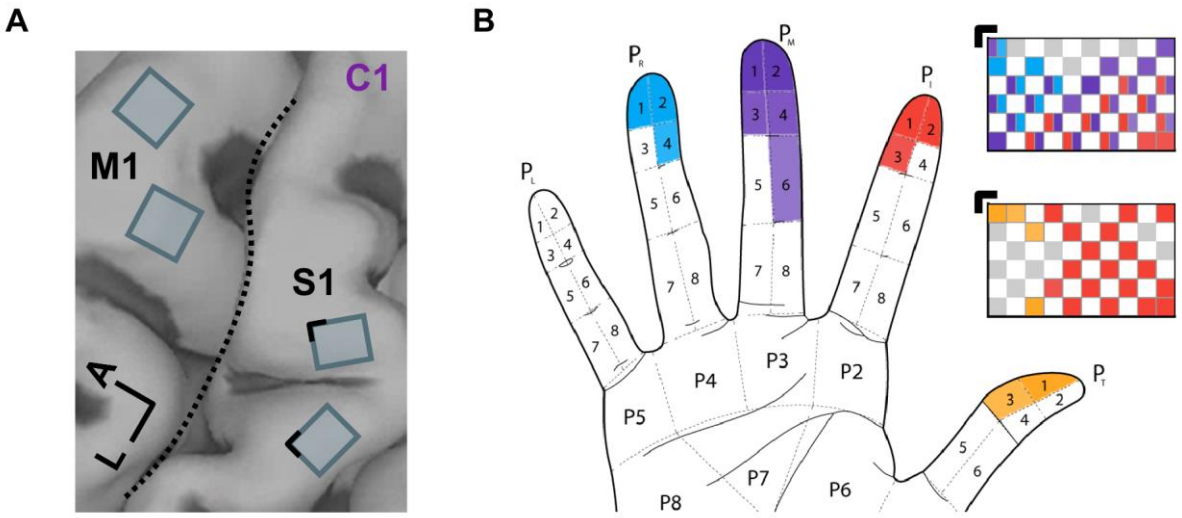

Figure 1. ICMS of S1 evokes tactile percepts whose location follows the expected somatotopic organization. A| Four Utah arrays (Blackrock Neurotech, Inc.) were implanted in participant C1, two of which were placed in the hand representation of S1, based on localization with fMRI. L: Lateral. A: Anterior. **B|** Locations of projected fields – the location on the hand where sensations are experienced – for each S1 channel for participant C1. The top array is medial, bottom one lateral. Colors denote the location of the projected field. Gray squares denote electrodes that evoked sensations on the dorsum of the hand, and white squares denote unwired electrodes. Black corners indicate alignment.

the range and precision of ICMS-based force feedback, we implemented "biomimetic" ICMS-trains, which, by emphasizing contact transients and de-emphasizing maintained contact, evoke patterns of neuronal activity that more closely mimic those in natural touch *(11, 12)*. We found that biomimetic ICMS yielded higher resolution force feedback than did its linear counterpart, even though the total charge of biomimetic ICMS spanned a narrower range. Next, we investigated whether we could further improve force feedback by delivering biomimetic ICMS through multiple electrodes simultaneously. We found that multi-channel biomimetic ICMS gives rise to stronger and more distinguishable sensations than does its single-channel counterpart, thus enabling precise force feedback over a wider range of forces. We conclude that biomimetic, multi-channel ICMS more closely approximates the sensitivity conferred by natural touch than does linear or biomimetic ICMS delivered through a single electrode.

RESULTS

Three participants with cervical spinal cord injury were each implanted with four electrode arrays, two in the arm and hand representation of motor cortex and two in the hand representation in Brodmann's area 1 of S1 (**Figure 1A**). In all three participants, stimulation through electrodes in S1 evoked sensations experienced on the contralateral hand, following the expected somatotopic organization (**Figure 1B** for C1, **Supplementary Figure 2A** for P2 and **Supplementary Figure 2B** for P3.).

The dynamic range of ICMS-evoked sensations is electrode dependent

In natural touch, increases in contact force lead to increases in the firing rate of active neurons and in the recruitment of additional neurons in a somatotopically determined region of S1 *(11)*. Increasing the ICMS amplitude leads to the same qualitative pattern of neuronal activation *(13)* and to increases in the perceived magnitude of the evoked sensation *(6–8)*, analogous to the sensory correlates of increases in

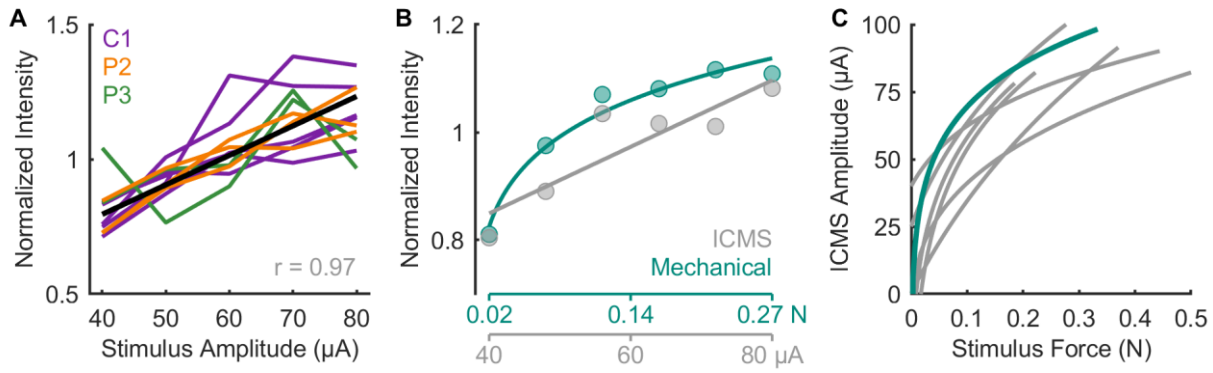

Figure 2. Perceived intensity increases linearly with ICMS amplitude. A| Normalized magnitude ratings following ICMS through single channels for 3 participants. Each line denotes ratings for one channel, different colors denote different participants. The thick black line denotes the mean across channels and participants. **B|** Normalized ratings when ICMS and mechanical stimuli are interleaved. **C|** Equal intensity contours for ICMS-evoked and mechanically evoked sensations. Each line represents the contour derived from the ratings from one stimulating channel. The teal line corresponds to the contour of the channel shown in panel B. While perceived magnitude increases with amplitude on all channels, the magnitude of the sensations varies widely across channels. Data from panels B and C are from participant C1 only.

pressure. With this in mind, we gauged the consistency of this relationship across participants and stimulating electrodes. The three participants rated the perceived magnitude of a sensation on a numerical scale of their choosing *(14)*. The ratings were then normalized by the mean rating for each electrode and their relationship with ICMS amplitude was characterized. On every electrode tested, perceived magnitude increased approximately linearly with ICMS amplitude, replicating previous findings (**Figure 2A**). The median correlation between amplitude and intensity rating was 0.97, with all but two correlations (both from participant P3) above 0.9 (range: 0.47 to 0.99). The relationship between ICMS amplitude and perceived magnitude is thus robust.

The limitation of the magnitude estimation approach, however, is that ratings are (by virtue of the paradigm) participant-specific *(14, 15)*, so they cannot be benchmarked to natural touch. Furthermore, ratings are normalized within each block or session so ratings cannot be compared across sessions. To overcome these limitations, we leveraged the fact that participant C1's tactile sensation on the hand is on par with that of able-bodied controls (**Supplementary Figure 2A,B**). Participant C1 judged the magnitude of the sensations evoked by ICMS trains and by skin indentations (delivered to a location matching the projected field of the stimulating electrode) of varying force, with the two types of stimuli interleaved randomly within each experimental block. We could then directly compare the magnitude of ICMS-evoked and mechanically evoked sensations (**Figure 2B**) because both stimulus types were rated on the same scale. Furthermore, assuming the perceived magnitude of the tactile stimuli remained constant across sessions, we could also compare the perceived magnitude of ICMS delivered through different electrodes on different sessions (**Supplementary Figure *2*B**). From these combined ICMS and touch sessions, we constructed equal intensity contours for the two stimulus types (**Figure 2C**), allowing us to determine the ICMS amplitude required to evoke a sensation whose intensity corresponds to a given force and vice-versa. First, we found that perceived magnitude increased approximately linearly with ICMS amplitude but as a (decelerating) power function of mechanical amplitude *(16)*(**Supplementary Figure 2C**). Accordingly, the iso-intensity contours also followed a power law, reflecting the non-linearity in the mechanically evoked sensations (**Figure 2C**). Furthermore, while the magnitude of ICMS-evoked sensations increased with amplitude on all electrodes, the intensity range of sensations varied widely

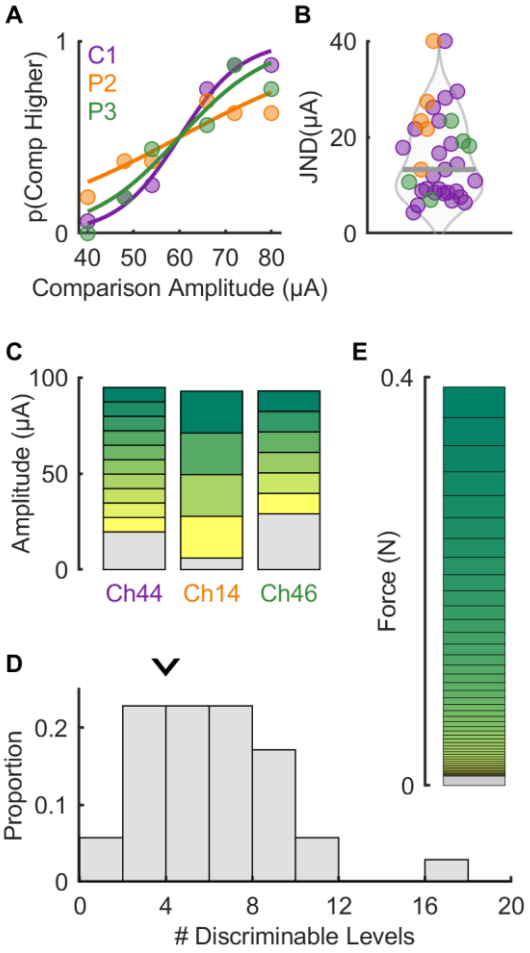

Figure 3. **Stimulus discriminability is electrode dependent.** **A|** Example psychometric functions from each participant – note that the curve for each participant is not representative of overall performance. **B|** JND computed from psychometric functions for all electrodes across participants (n = 35) – thick grey line denotes median (13.5 μA). Note that values above 40 μA are set to 40 μA for graphical purposes (n=2). **C|** Estimated discriminable levels plots for the electrodes shown in panel A. The grey section at the bottom of each bar indicates the subthreshold range for that electrode while the height of each subsequent bar is determined by the JND. **D|** The number of discriminable levels across all electrode and participants. Arrow indicates median number of discriminable levels (4). **E|** Estimated discriminable levels for tactile stimulation in the same approximate range of forces (0-0.4N). Note that JNDs increase for higher force levels following Weber's law.

across electrodes: some electrodes could only evoke weak sensations (< 0.3 N, the weight of a marshmallow balanced on a finger), whereas others could evoke sensations commensurate with moderate forces (~ 0.5 N, the weight of an egg). Given that contact forces often exceed 1 N during object interactions *(17, 18)*, the dynamic range of ICMS-evoked sensations, constrained by the maximum safe stimulation level (100 μA, *(6, 19)*), is generally narrow.

The discriminability of evoked percepts is electrode dependent

Having established that the mapping between ICMS amplitude and perceived contact force was electrode dependent, we investigated how sensitive participants were to changes in ICMS amplitude. To this end, we had participants discriminate flat ICMS trains that varied in amplitude. In brief, we presented two stimuli – a reference stimulus at 60 μA and a comparison whose amplitude varied between 40 and 80 μA – and the participant reported which of the two was more intense. From the behavioral performance, (**Figure 3A**), we computed, as an index of sensitivity for each electrode, the Just Noticeable Difference (JND), which denotes the change in stimulus amplitude that would yield a criterion level of performance (75% correct). While the median JND was around 13.5 μA (**Figure 3B**), consistent with previous results in humans and monkeys *(6, 7, 9, 10)*, JNDs varied widely across electrodes and participants (interquartile range: 8.5 to 22.9 μA). Having measured the detection threshold and the JND for each electrode, we computed the number of discriminable levels (**Figure 3C**), defined as the number of JNDs between detection threshold and maximum safe amplitude (100 μA). Note that ICMS does not follow Weber's law *(6, 10)* so the JND measured for each electrode at any amplitude applies across the range of amplitudes. We found that the number of discriminable steps ranged from 2 to 17, with a median of 4 (**Figure 3D**), implying that the force feedback conveyed by flat ICMS is coarse, allowing for only a handful of discriminable levels within the safe stimulation range. Electrodes with lower detection thresholds tended to have higher JNDs ($r = -0.51$, $p < 0.01$, **Supplementary Figure 3A**), suggesting that JNDs do not simply reflect overall sensitivity to ICMS. Electrodes with more discriminable levels also

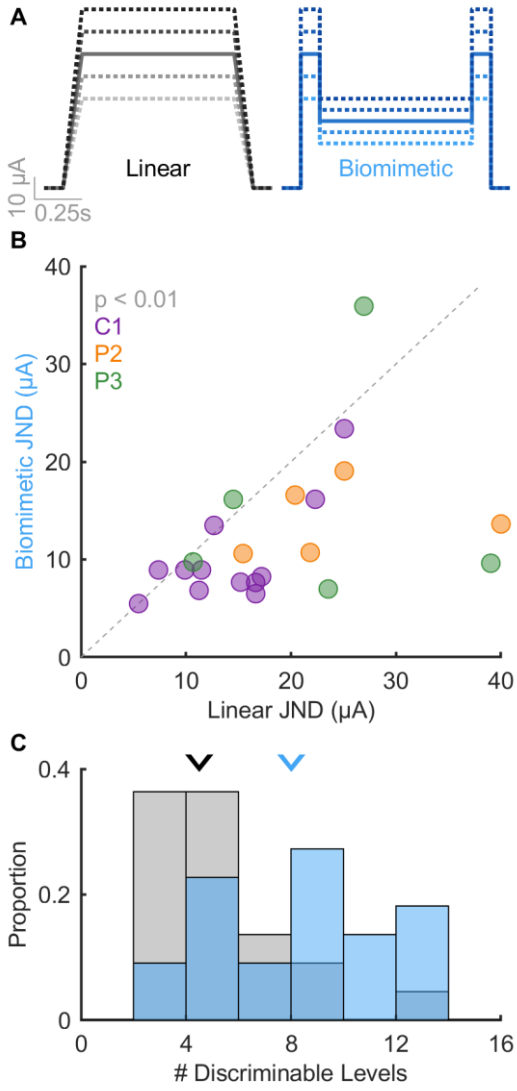

Figure 4. Biomimetic stimuli are more discriminable than linear stimuli. A| Example idealized stimulus profiles for linear (where stimulus amplitude scales with force) and biomimetic (where force transients are emphasized) stimuli. **B|** JNDs are reduced (sensitivity enhanced) with biomimetic stimuli versus linear ones. **C|** The distribution of the number of discriminable levels computed from JNDs with linear (gray) or biomimetic (blue) stimuli. The number of levels increases with biomimetic stimuli versus linear ones (median = 8 vs. 5, respectively).

tended to evoke the most intense sensations (r = 0.87, p = 0.02, **Supplementary Figure *3*B**), implying that the JND for each electrode corresponds with a change in intensity that is approximately consistent across electrodes, a phenomenon that is non-trivial given that magnitude functions are not systematically predictable from JNDs in natural perception *(20, 21)*. As a point of comparison, the native touch of both participant C1 and able-bodied controls (n = 5) yielded around 45-50 discriminable levels over this span of forces, an order of magnitude more than what could be achieved with single-channel ICMS over the safe range of amplitudes (**Figure 3E**).

Biomimetic feedback confers greater sensitivity to force changes

In the experiments described above, ICMS consisted of pulse trains of constant amplitude (flat trains). Such pulse trains typically evoke an abrupt rise in the activation of neurons around the electrode, followed by a slow decrease *(22)*. In contrast, interactions with objects evoke phasic responses at the onset and offset of contact and much weaker responses (< 10%) during maintained contact, a property inherited from the periphery *(11)*. In studies with electrical stimulation of the peripheral nerves, tactile feedback that features greater sensitivity to contact transients (thereby mimicking natural touch) has been shown to confer greater dexterity to myoelectric bionic hands *(23–25)*. With this in mind, we assessed participants' ability to discriminate biomimetic ICMS trains, designed to mimic the response to the onset, maintenance, and termination of contact (**Figure 4A**). We compared the participants performance with biomimetic trains to that with trains designed to track the forces linearly, which largely resembled flat trains with short on- and off-ramps. For this comparison, the biomimetic and linear trains were matched in peak amplitude; as a result, the charge delivered in a biomimetic train was less than that in a matched linear one (69 ± 7 % on average, see Methods). We found that JNDs for biomimetic ICMS were systematically lower than were their linear counterparts (**Figure 4B**, medians: 9.7 and 16.6 µA; IQRs: 7.7 to 16.1 µA and 11.5 to 23.5 µA, respectively, Wilcoxon signed-rank test, n = 22, z = 3.1, p < 0.01). The

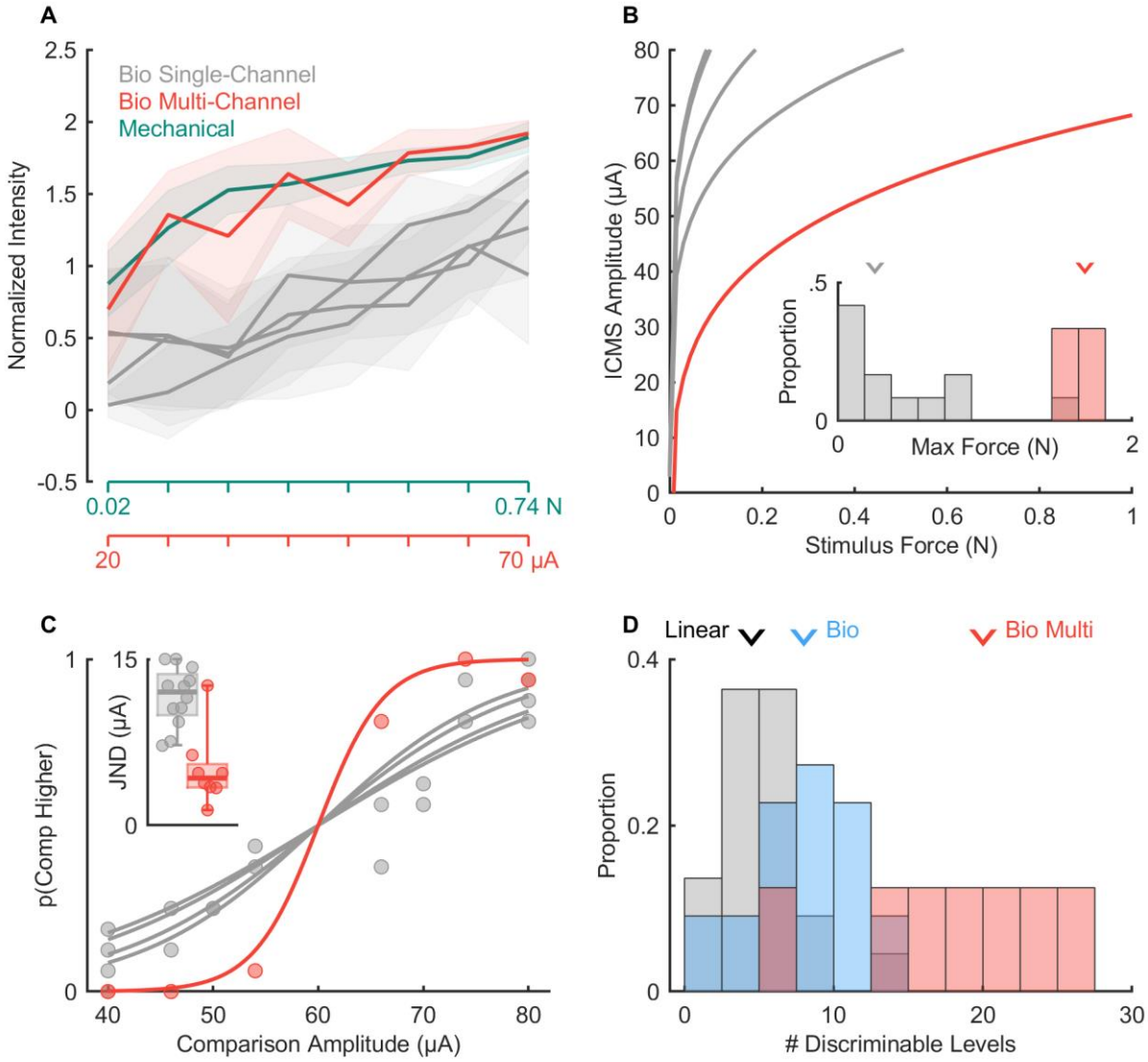

Figure 5. Multi-channel biomimetic stimulation produces more intense and more discriminable percepts. A| Normalized magnitude ratings when ICMS is delivered through electrodes individually or simultaneously, interleaved with mechanical stimuli for an example quad. All ICMS trains were biomimetic (cf. **Figure 4A)**. Lines denote the mean while shaded areas denote the standard deviation. **B|** Iso-intensity contours for single-channel (gray) and multi-channel (red) ICMS for an example quad. Inset: Maximum achievable force for single or multi-channel stimulation across all tested quads, extrapolating fits to 100 µA. **C|** Psychometric functions for one quad of electrodes with the performance of the individual electrodes shown in gray and that of the quad in red. Inset: JNDs for all single electrodes and quads tested. The median JND decreased from 12 to 4.3 µA with multi-channel ICMS (Wilcoxon rank sum test: $Z = -3.05$, $p < 0.01$). **D|** Estimated number of discriminable levels with single-channel ICMS (linear or biomimetic stimuli, median = 4.5 and 8, cf. **Figure 4C**) and multi-channel biomimetic ICMS (median = 20). Panels A & B show results from participant C1 while panels C & D show results from participants C1 and P2.

improved sensitivity to biomimetic ICMS is especially surprising given that biomimetic trains contained less charge. For the set of electrodes tested in this comparison, the median number of discriminable levels increased from 4.5 to 8 with biomimetic sensory feedback (**Figure 4C**). Biomimetic ICMS trains thus provide higher resolution force feedback, an advantage that is even more pronounced when expressed in

terms of charge rather than peak amplitude (**Supplementary Figure *4*A,B**) and does not reflect differences in perceived intensity (**Supplementary Figure *4*C**).

Multi-channel feedback confers greater dynamic range and change sensitivity

Having characterized the dynamic range and resolution of ICMS-based force feedback delivered through single-channel at a time, we next examined the magnitude of sensations evoked when ICMS was delivered through multiple electrodes simultaneously. For these experiments, we selected groups of 4 electrodes (quads) with overlapping or adjacent projected fields (the hand regions over which the sensations were experienced) (**Supplementary Figure 5A**). That is, when stimulation was delivered through each of the four electrodes individually, the sensation was experienced on an overlapping patch of skin or, in one case, on adjacent digits. In these experiments, ICMS was always biomimetic, comprising higher amplitude phasic stimulation at the onset and offset and weaker stimulation between the two phasic components. First, we assessed whether multi-channel stimulation increased the dynamic range of the evoked sensations by comparing magnitude estimates of intensity with (biomimetic) single- vs. multi-channel stimulation (3 sets of 4 electrodes in participant C1). We found that multi-channel stimulation evoked systematically more intense sensations than did single-channel stimulation when equating the current delivered through each electrode individually (so quad stimulation delivered four times more total current than did its matched single-electrode counterpart, **Figure 5A**). Nonetheless, within the safe range of ICMS amplitudes, multi-channel ICMS allowed for a much wider dynamic range than did any electrode in isolation (more than twice the average electrode, **Figure 5B**). Indeed, the peak equivalent force reached 2 N, approximately the weight of a mobile phone. Furthermore, the multi-channel ICMS amplitude intensity function still followed a linear relationship with amplitude (**Supplementary Figure *5*B**) so this linear relationship is not an artifact of a narrow range of intensities *(20)*.

Next, we examined the discriminability of multi-channel biomimetic ICMS trains that varied in amplitude (n = 8 quads, 5 from participant C1 and 3 from participant P2). We found that multi-channel ICMS yielded substantially lower JNDs than did its single-channel counterpart (**Figure 5C**), mirroring the lower variability in the magnitude estimates of intensity for multi-channel stimulation compared to its single channel counterpart (**Supplementary Figure 5D**). Combined, the wider dynamic range and higher resolution yielded an increase in the median number of discriminable levels from 8 to 20 (**Figure 5D**). Thus, biomimetic multi-channel force feedback can yield more precise force feedback over a wider dynamic range than does standard force feedback through a single electrode. Indeed, while JNDs expressed in terms of charge were equivalent or higher for multi-channel than single-channel stimulation (**Supplementary Figure *5*C**), the bottleneck in ICMS-based feedback is the charge delivered on any given electrode, which is the primary determinant of stimulation-induced neuronal damage *(26)*. Multi-channel ICMS circumvents this limitation by distributing charge, thereby increasing both the range and precision of the resulting sensations to a level that more closely approximates natural touch (~20 vs. 45-50 discriminable steps, respectively).

DISCUSSION

Biomimetic ICMS confers higher resolution force feedback

The rationale behind biomimetic feedback is that it evokes more natural patterns of neural activation, which then gives rise to more easily interpretable sensations *(27, 28)*. In experiments with human amputees, biomimetic sensory feedback has been shown to improve the function of myoelectric bionic

hands *(23, 24)*: With biomimetic feedback, users could more rapidly transfer fragile objects or identify the compliance of objects. However, JNDs were higher with biomimetic feedback, suggesting that the intuitiveness of the biomimetic feedback made up for its lower resolution. Note, however, that this was demonstrated on a single channel and therefore should be replicated before definitive conclusions can be drawn given the channel-dependence of the effect observed with peripheral nerve stimulation *(23)*. For ICMS-based feedback, biomimetic trains differing in amplitude are even more discriminable than are their amplitude-matched linear trains. The difference between biomimetic and linear ICMS trains is even more pronounced when the stimulation intensity is expressed in terms of overall charge (**Supplementary Figure *4*B**). Whether biomimetic ICMS leads to more intuitive sensations has yet to be systematically investigated, though preliminary findings are promising *(29)*. Regardless, biomimetic ICMS-based feedback offers the additional advantage of higher resolution force information, unlike its peripheral counterpart.

Multi-channel ICMS confers wider dynamic range and higher resolution

Multi-channel ICMS leads to more intense sensations than single-channel ICMS. This finding is perhaps unsurprising given that multi-channel stimulation entails four times more charge delivery than does single-channel stimulation. In fact, multi-channel stimulation less efficiently modulates the overall perceived magnitude compared to single-channel stimulation when expressed as a function of overall charge (**Supplementary Figure 5B**). The major bottleneck in ICMS-based sensory feedback, however, is that the amplitude used in human experiments is capped at 100 μA, as this level of stimulation has been shown in experiments with monkeys to cause no damage beyond that incurred during implantation *(30)*. Even if this maximum level turns out to be more conservative than it needs to be, evidence suggests that charge per phase is the main determinant of ICMS-induced neuronal damage *(26)*. Accordingly, multi-channel ICMS enables a widening of the dynamic range without increasing the charge per phase on any given electrode.

Beyond widening the dynamic range, multi-channel ICMS improved the resolution of the feedback, as gauged by lower JNDs. While a reduction in detection thresholds and quickened reaction times with multi-channel stimulation has been previously reported in both humans *(31)* and monkeys *(32, 33)*, the improvement in discriminability has not. In fact, this improvement is inconsistent with the results of experiments with monkeys, in which multi-channel ICMS yielded similar JNDs as did its single-channel counterpart *(34)*. The basis for this discrepancy is unclear. One major difference between this study and the other, however, is that all the electrodes were adjacent in the experiments with monkeys, whose hand representation in S1 is almost an order of magnitude smaller than its human counterpart, whereas the electrodes were often non-adjacent in the present experiment with humans (the only requirement being that they had at least partially overlapping projected fields). Adjacent electrodes are liable to excite overlapping populations of neurons whereas non-adjacent ones are not *(35)*. Stimulation through non-adjacent electrodes is thus likely to recruit more neurons with increases in amplitude than is stimulation through non-adjacent electrodes. This difference between the experiments with humans and monkeys may explain the discrepant effect of multi-channel stimulation on JNDs.

While JNDs are lower for multichannel biomimetic stimulation, each JND leads to a greater increment in perceived magnitude. As a result, while the resolution of multichannel stimulation is higher for ICMS amplitude, it is equivalent for force. Indeed, successive discriminable increments in amplitude are associated with larger increments in force with multichannel stimulation to maintain a correspondence

between the level of force exerted and the sensory experience. However, the dynamic range of forces is much higher for multichannel than single channel stimulation.

CONCLUSIONS

Biomimetic multi-channel stimulation doubles the dynamic range of the evoked touch sensations, decreases the JNDs, and yields nearly fivefold more discriminable levels of force than does single-channel linear feedback. Biomimetic trains yield more discriminable percepts and do so more efficiently, in terms of charge. While multi-channel stimulation is not more efficient than is its single channel counterpart, distributing charge across electrodes increases the dynamic range without increasing the charge density, which is the main determinant of stimulation-induced neuronal damage.

METHODS

Participants

This study was conducted under an Investigational Device Exemption from the U.S. Food and Drug Administration and approved by the Institutional Review Boards at the University of Pittsburgh and the University of Chicago. The clinical trial is registered at ClinicalTrials.gov (NCT01894802). Informed consent was obtained before any study procedures were conducted. Participant C1 (m), 57 years old at the time of implant, presented with a C4-level ASIA D spinal cord injury (SCI) that occurred 35 years prior to implant. Participant P2 (m), 28 years old at the time of implant, presented with a C5 motor/C6 sensory ASIA B SCI that occurred 10 years prior to implant. Participant P3 (m), 28 years old at the time of implant, presented with a C6 ASIA B SCI that occurred 12 years prior to implant.

Cortical implants

We implanted four microelectrode arrays (Blackrock Neurotech, Salt Lake City, UT, USA) in each participant. The two arrays (one medial and one lateral array) in Brodmann's area 1 of somatosensory cortex and were 2.4 mm x 4 mm with sixty 1.5-mm long electrode shanks wired in a checkerboard pattern such that 32 electrodes could be stimulated. The two arrays in primary motor cortex were 4 mm x 4 mm with one-hundred 1.5-mm long electrode shanks wired such that 96 (C1 and P3) or 88 (P2) electrodes could measure neural activity. The inactive shanks were located at the corners of these arrays. Two percutaneous connectors, each connected to one sensory array and one motor array, were fixed to the participant's skull. We targeted array placement during surgery based on functional neuroimaging (fMRI) of the participants attempting to make movements of the hand and arm (all participants) and imagining feeling sensations on their fingertips (participant P2), within the constraints of anatomical features such as blood vessels and cortical topography.

Intracortical microstimulation (ICMS)

Stimulation was delivered via a CereStim 96 (Blackrock Neurotech). Each stimulating pulse consisted of a 200 μs cathodic phase followed by a half-amplitude 400 μs anodic phase (to maintain charge balance), the two phases separated by 100 μs. In all tasks, conditions were interleaved, counterbalanced when appropriate, and randomized within block.

Multi-channel ICMS

We selected groups of 4 electrodes, referred to as quads. In most cases, the four electrodes had overlapping projected fields. In one case, one pair of electrodes in the quad were on one digit and the other pair was on the adjacent digit. During an experimental block, we randomly interleaved stimulation through each channel in each quad with stimulation through the entire quad. For multi-channel ICMS, an identical pulse train was delivered through every channel of the quad.

Mechanical skin indentation

To deliver mechanical indentations into the skin of participant C1, we used a V-308 voice coil (Physik Instrumente, USA, MA) to drive an indenter whose tip was 5 mm in diameter. Stimuli were 1 second in duration with 0.1 second ramps, matching the profile of the ICMS, and ranged in amplitude from 0.02 mm to 2 mm. The tip was centered on the location of the projected field for a given electrode as reported by the participant. The indenter tip was then pre-indented into the skin to ensure maintained contact throughout the experimental block. Mechanical indentations were also delivered to five able-bodied participants (all male, 24-33 years of age) under a separate IRB protocol approved by the University of Chicago.

Amplitude discrimination

Participants performed an amplitude discrimination task in a two-alternative forced choice paradigm. On each trial, a pair of stimuli, each lasting 1 second, was presented with a 1second inter-stimulus interval and the participant reported which stimulus was stronger. The reference stimulus, consistent across the experimental block, was paired with a comparison stimulus whose amplitude varied from trial to trial. The order of presentation of the reference and comparison stimuli was randomized and counterbalanced. Data were obtained from each electrode over a minimum of 8 experimental blocks, each consisting of 2 presentations (one for each order) for each stimulus pair.

The frequency of the ICMS stimuli was either 50 Hz (**Figure 3**) or 100 Hz (all other experiments). For linear ICMS, two trapezoidal force traces (see force approximation below) were generated (0.1 second ramps and 0.8 second hold) and converted into trains of ICMS that followed the force trace and peaked at an amplitude proportional to the peak force. Biomimetic stimuli consisted of a transient phase – whose duration matched that of the force ramp (0.1 sec) and whose pulse amplitude matched that of the corresponding linear train – and a hold phase during the static component of the force (0.8 sec), during which the pulse amplitude was either 30 µA less than the amplitude in the transient phase or at the detection threshold, whichever was highest. On any given experimental block, the reference amplitude was 60 µA and the comparison stimuli varied in amplitude between 40 and 80 µA (**Figure 4A**). Note that the JNDs were the same at 50 and 100 Hz, as has been previously found in experiments with monkeys *(10)*.

The same paradigm was used to measure amplitude JNDs with the mechanical indenter as for ICMS. The indentation depths varied between 0.85 and 1.15 mm with a standard amplitude of 1 mm and the onset- and offset-ramp speed was 5 mm/s.

Magnitude estimation

In this task, participant C1 rated the perceived magnitude of an ICMS train (single- or multi-channel) or mechanical indentation. Briefly, on each trial, the participant was presented with an ICMS or a mechanical stimulus (queued with a fixation cross) and rated its sensory magnitude on a scale of his choosing. If the

stimulus was imperceptible, the participant ascribed to it a rating of zero. If one stimulus was twice as intense as another, it was ascribed a rating that was twice as large. The participant was encouraged to use fractions or decimals. At the beginning of each set, the participant was presented with each of the test stimuli in a random order to familiarize them with the stimulus range. The amplitude of the ICMS stimulus varied between 20 and 80 µA while the mechanical stimuli ranged from 0.05 to 2 mm. In all cases the mechanical stimulus was delivered to the location of the projected field for the given electrode. Both ICMS and mechanical stimuli were interleaved throughout each block, with a 5-sec interstimulus interval.

In experimental blocks involving both skin indentations and ICMS, the range of indentation depths was selected in preliminary measurements to match the range of intensities of the electrical stimuli (based on participant ratings) to maximize the overlap and minimize range-related biases. To this end, we estimated, at the start of the session and with the participants help, the range of mechanical indentations that evoked sensations of comparable intensity as their ICMS counterparts (which varied from channel to channel). When multiple channels were tested, we selected the weakest and strongest sensations across channels. We then evenly sampled intermediate indentation depths between these two extremes. In some cases, the intensity of the multi-channel ICMS exceeded the maximum indentation that could be delivered with the indenter, precluding comparisons at higher amplitudes.

A minimum of 8 blocks were completed for each channel and condition. Blocks were sometimes distributed across several days to minimize the effects of adaptation *(36)* and maintain participant engagement.

Detection thresholds

Detection thresholds were measured separately on a quarterly basis as described previously *(6)*. We either used a 3 up 1 down transformed staircase or the method of limits – both in a 2-alternate forced choice (AFC) design targeting 50% detection performance.

Projected fields

Projected fields were collected over multiple years for each electrode and participant. On each trial, a 60-µA, 100-Hz ICMS train was delivered through a given electrode and the participant drew the spatial extent of the sensation on a hand diagram (such as that shown in Figure 1B) using a tablet. The region enclosed by the drawn boundary constituted an estimate of the projected field for that electrode on that session. Only hand regions that were included in the projected field on two thirds of the sessions were included in the pooled estimate of the projected field.

Analysis

Iso-intensity contours

From magnitude ratings obtained when both skin indentation and ICMS were interleaved, we fit a power function to the magnitude ratings, M_m, for skin indentations of amplitude a_m:

$$M_m = \alpha a_m^{\gamma}$$

and a linear function to the magnitude ratings, M_e, of ICMS of amplitude a_e:

$$M_e = \beta a_e$$

We then derived an equal intensity contour for stimuli of equal perceived magnitude, where $M_m = M_e$:

$$a_e = \frac{\alpha}{\beta} a_m^{\gamma}$$

Force approximation

To convert skin indentations into equivalent forces, we measured the relationship between skin indentation and exerted force using a Universal Testing Machine (Instron, **Supplementary Figure 6**). Data was collected from 15 individuals (8 women, 7 men) aged between 21 and 30. We then used this measured function to estimate the forces in the magnitude estimation task.

Psychometric functions

Psychometric functions were fit with a logistic function:

$$p = \frac{1}{1 + e^{k*(x-\mu)}}$$

Where p is the probability of judging the comparison stimulus as more intense than the reference, x is the amplitude, k is the slope, and μ the point of subjective equality (PSE). The just noticeable difference (JND) is half the difference between the amplitude that yields a p of 0.75 and the amplitude that yields a p of 0.25.

Discriminable levels

To estimate the number of discriminable levels for ICMS we used the formula:

$$DL = \frac{100 - dt_{50}}{JND}$$

where DL is the number of discriminable levels, dt_{50} is the 50% detection threshold for the channel, and JND is the Just Noticeable Difference for that channel.

To estimate the number of discriminable levels for mechanical stimulation, we computed the Weber fraction from the amplitude discrimination experiment and used a detection threshold of 0.05 µm, estimated from the magnitude estimation experiments. We then extrapolated the discriminable levels until we reached the amplitude whose perceived magnitude matched that of the ICMS at maximum amplitude.

REFERENCES

1. R. S. Johansson, J. R. Flanagan, Coding and use of tactile signals from the fingertips in object manipulation tasks. *Nature Reviews Neuroscience* **10**, 345–359 (2009).

2. R. S. Johansson, G. Westling, Signals in tactile afferents from the fingers eliciting adaptive motor responses during precision grip. *Exp Brain Res* **66**, 141–154 (1987).

3. J. Monzée, Y. Lamarre, A. M. Smith, The Effects of Digital Anesthesia on Force Control Using a Precision Grip. *Journal of Neurophysiology* **89**, 672–683 (2003).

4. S. J. Bensmaia, D. J. Tyler, S. Micera, Restoration of sensory information via bionic hands. *Nature Biomedical Engineering* , 1–13 (2020).

5. C. Pandarinath, S. J. Bensmaia, The science and engineering behind sensitized brain-controlled bionic hands. *Physiological Reviews* **102**, 551–604 (2022).

6. S. N. Flesher, J. L. Collinger, S. T. Foldes, J. M. Weiss, J. E. Downey, E. C. Tyler-Kabara, S. J. Bensmaia, A. B. Schwartz, M. L. Boninger, R. A. Gaunt, Intracortical microstimulation of human somatosensory cortex. *Science Translational Medicine* **8**, 361ra141-361ra141 (2016).

7. M. A. Salas, L. Bashford, S. Kellis, M. Jafari, H. Jo, D. Kramer, K. Shanfield, K. Pejsa, B. Lee, C. Y. Liu, R. A. Andersen, Proprioceptive and cutaneous sensations in humans elicited by intracortical microstimulation. *eLife* **7**, 1–11 (2018).

8. S. N. Flesher, J. E. Downey, J. M. Weiss, C. L. Hughes, A. J. Herrera, E. C. Tyler-Kabara, M. L. Boninger, J. L. Collinger, R. A. Gaunt, A brain-computer interface that evokes tactile sensations improves robotic arm control. *Science* **372**, 831–836 (2021).

9. G. A. Tabot, J. F. Dammann, J. A. Berg, F. V. Tenore, J. L. Boback, R. J. Vogelstein, S. J. Bensmaia, Restoring the sense of touch with a prosthetic hand through a brain interface. *Proceedings of the National Academy of Sciences* **110**, 18279–18284 (2013).

10. S. Kim, T. Callier, G. A. Tabot, R. A. Gaunt, F. V. Tenore, S. J. Bensmaia, Behavioral assessment of sensitivity to intracortical microstimulation of primate somatosensory cortex. *Proc. Natl. Acad. Sci. U.S.A.* **112**, 15202–15207 (2015).

11. T. Callier, A. K. Suresh, S. J. Bensmaia, Neural Coding of Contact Events in Somatosensory Cortex. *Cerebral Cortex* **29**, 4613–4627 (2019).

12. C. Hughes, T. Kozai, Biomimetic microstimulation of sensory cortices. *bioRxiv* , 2022–11 (2022).

13. K. Kumaravelu, J. Sombeck, L. E. Miller, S. J. Bensmaia, W. M. Grill, Stoney vs. Histed - Quantifying the Spatial Effects of Intracortical Microstimulation. *bioRxiv* , 2021.08.12.456091 (2021).

14. G. A. Gescheider, *Psychophysics: The fundamentals* (Lawrence Erlbaum Associates Publishers, Mahwah, NJ, US, ed. 3rd, 1997), pp. x, 435.

15. E. C. Poulton, The new psychophysics: Six models for magnitude estimation. *Psychological Bulletin* **69**, 1–19 (1968).

16. S. S. Stevens, On the psychophysical law. *Psychological Review* **64**, 153–181 (1957).

17. G. Westling, R. S. Johansson, Factors influencing the force control during precision grip. *Experimental Brain Research* **53** (1984), doi:10.1007/BF00238156.

18. G. Westling, R. S. Johansson, Responses in glabrous skin mechanoreceptors during precision grip in humans. *Exp Brain Res* **66**, 128–140 (1987).

19. C. L. Hughes, S. N. Flesher, J. M. Weiss, J. E. Downey, M. Boninger, J. L. Collinger, R. A. Gaunt, Neural stimulation and recording performance in human sensorimotor cortex over 1500 days. *J. Neural Eng.* **18**, 045012 (2021).

20. R. Teghtsoonian, On the exponents in Stevens' law and the constant in Ekman's law. *Psychological Review* **78**, 71–80 (1971).

21. L. E. Krueger, Reconciling Fechner and Stevens: Toward a unified psychophysical law. *Behavioral and Brain Sciences* **12**, 251–267 (1989).

22. M. C. Dadarlat, Y. J. Sun, M. P. Stryker, Spatiotemporal recruitment of inhibition and excitation in the mammalian cortex during electrical stimulation. *bioRxiv* , 2022.06.03.494729 (2022).

23. G. Valle, A. Mazzoni, F. Iberite, E. D'Anna, I. Strauss, G. Granata, M. Controzzi, F. Clemente, G. Rognini, C. Cipriani, T. Stieglitz, F. M. Petrini, P. M. Rossini, S. Micera, Biomimetic Intraneural Sensory Feedback Enhances Sensation Naturalness, Tactile Sensitivity, and Manual Dexterity in a Bidirectional Prosthesis. *Neuron* **100**, 37-45.e7 (2018).

24. J. A. George, D. T. Kluger, T. S. Davis, S. M. Wendelken, E. V. Okorokova, Q. He, C. C. Duncan, D. T. Hutchinson, Z. C. Thumser, D. T. Beckler, P. D. Marasco, S. J. Bensmaia, G. A. Clark, Biomimetic sensory feedback through peripheral nerve stimulation improves dexterous use of a bionic hand. *Science Robotics* **4**, eaax2352 (2019).

25. M. Aboseria, F. Clemente, L. F. Engels, C. Cipriani, Discrete Vibro-Tactile Feedback Prevents Object Slippage in Hand Prostheses More Intuitively Than Other Modalities. *IEEE Transactions on Neural Systems and Rehabilitation Engineering* **26**, 1577–1584 (2018).

26. D. McCreery, M. Han, V. Pikov, C. Miller, Configuring intracortical microelectrode arrays and stimulus parameters to minimize neuron loss during prolonged intracortical electrical stimulation. *Brain Stimulation* **14**, 1553–1562 (2021).

27. H. P. Saal, S. J. Bensmaia, Biomimetic approaches to bionic touch through a peripheral nerve interface. *Neuropsychologia* **79**, 344–353 (2015).

28. E. V. Okorokova, Q. He, S. J. Bensmaia, Biomimetic encoding model for restoring touch in bionic hands through a nerve interface. *Journal of neural engineering* **15**, 066033 (2018).

29. C. L. Hughes, J. M. Weiss, S. J. Bensmaia, R. A. Gaunt, in *Society for Neuroscience Abstracts*, (Chicago, 2018), p. 404.05.

30. A. T. Rajan, J. L. Boback, J. F. Dammann, F. V. Tenore, B. A. Wester, K. J. Otto, R. A. Gaunt, S. J. Bensmaia, The effects of chronic intracortical microstimulation on neural tissue and fine motor behavior. *J. Neural Eng.* **12**, 066018 (2015).

31. D. A. Bjånes, L. Bashford, K. Pejsa, B. Lee, C. Y. Liu, R. A. Andersen, Multi-channel intra-cortical micro-stimulation yields quick reaction times and evokes natural somatosensations in a human participant. *medRxiv* , 2022.08.08.22278389 (2022).

32. B. Zaaimi, R. Ruiz-Torres, S. A. Solla, L. E. Miller, Multi-electrode stimulation in somatosensory cortex increases probability of detection. *J. Neural Eng.* **10**, 056013 (2013).

33. J. Sombeck, L. E. Miller, Short reaction times in response to multi-electrode intracortical microstimulation may provide a basis for rapid movement-related feedback. *Journal of neural engineering* , 1–27 (2019).

34. S. Kim, T. Callier, G. A. Tabot, F. V. Tenore, S. J. Bensmaia, Sensitivity to microstimulation of somatosensory cortex distributed over multiple electrodes. *Frontiers in Systems Neuroscience* **10**, 47 (2015).

35. S. D. Stoney, W. D. Thompson, H. Asanuma, Excitation of pyramidal tract cells by intracortical microstimulation: effective extent of stimulating current. *Journal of Neurophysiology* **31**, 659–669 (1968).

36. C. L. Hughes, S. N. Flesher, R. A. Gaunt, *Effects of stimulus pulse rate on somatosensory adaptation in the human cortex* (2021; https://www.biorxiv.org/content/10.1101/2021.12.04.471210v1), p. 2021.12.04.471210.

SUPPLEMENTARY FIGURES

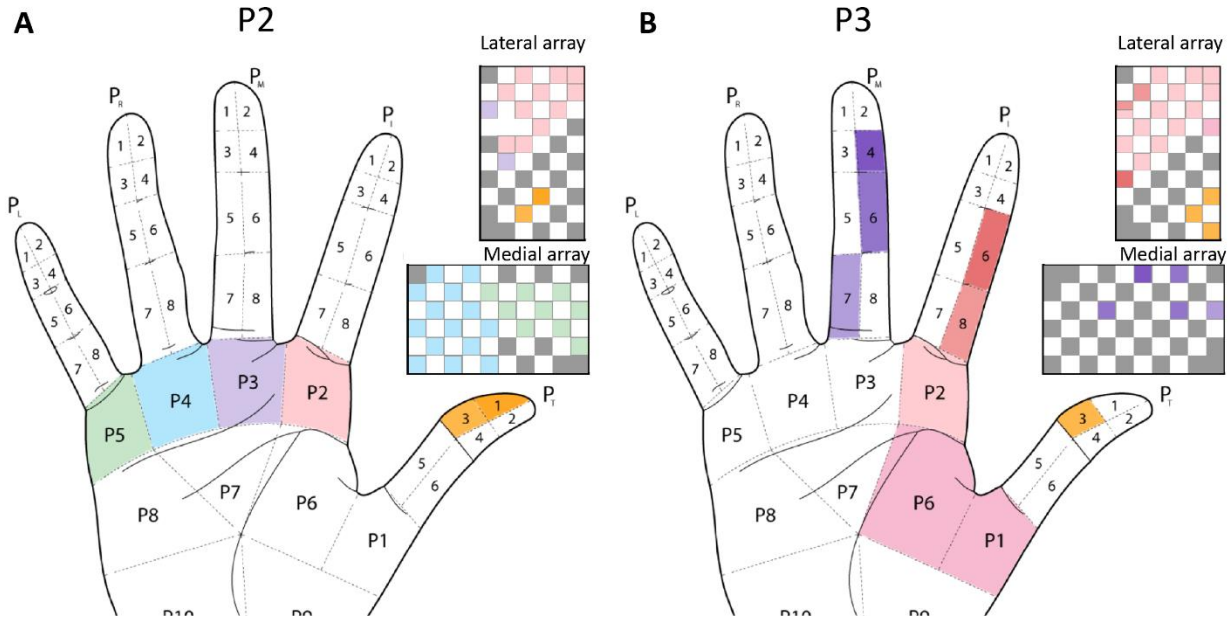

Supplementary Figure 1. A| Locations of projected fields – the location on the hand where sensations are experienced – for each S1 channel for participant P2. **B|** Locations of projected fields – the location on the hand where sensations are experienced – for each S1 channel for participant P3. The top array is medial, bottom one lateral. Colors denote the location of the projected field. Gray squares denote electrodes that evoked sensations on the dorsum of the hand, and white squares denote unwired electrodes.

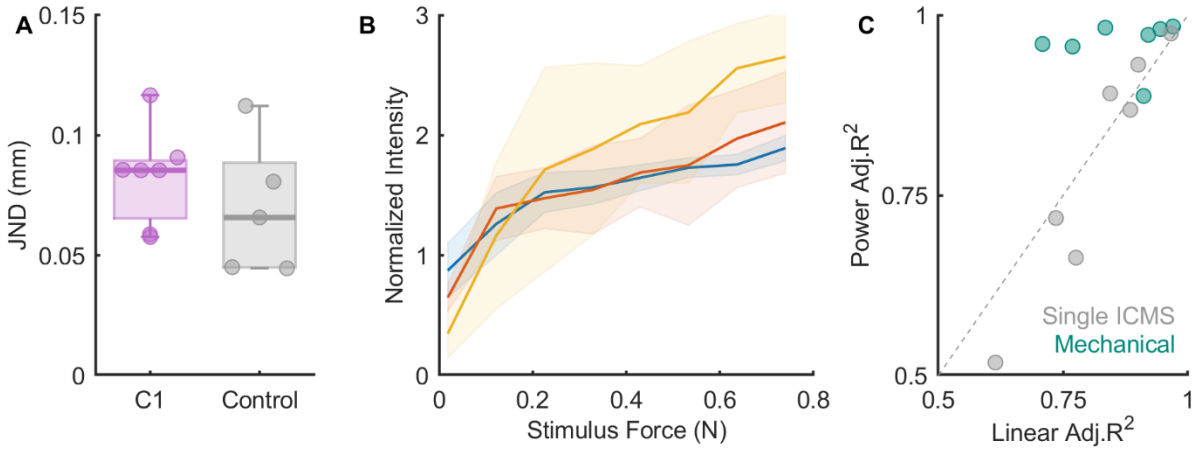

Supplementary Figure 2. A| Mechanical JNDs for participant C1 (each point denotes performance on an individual digit) and for 5 able-bodied controls (each point denotes performance of one participant on the tip of the middle finger). The participant's ability to distinguish the depth of indentation is comparable to that of the controls. **B|** Normalized intensity ratings from participant C1 on 3 different fingers (denoted by different colors). Ratings are consistent across fingers. Note that the normalization was performed based on the grand mean rating, which included ratings of single-channel ICMS stimuli and tended to be weaker than the mechanical ones. **C|** Goodness of fit for ICMS or mechanical intensity ratings when using power vs. linear functions. Power functions provide better fits for intensity ratings of skin indentations but not ICMS.

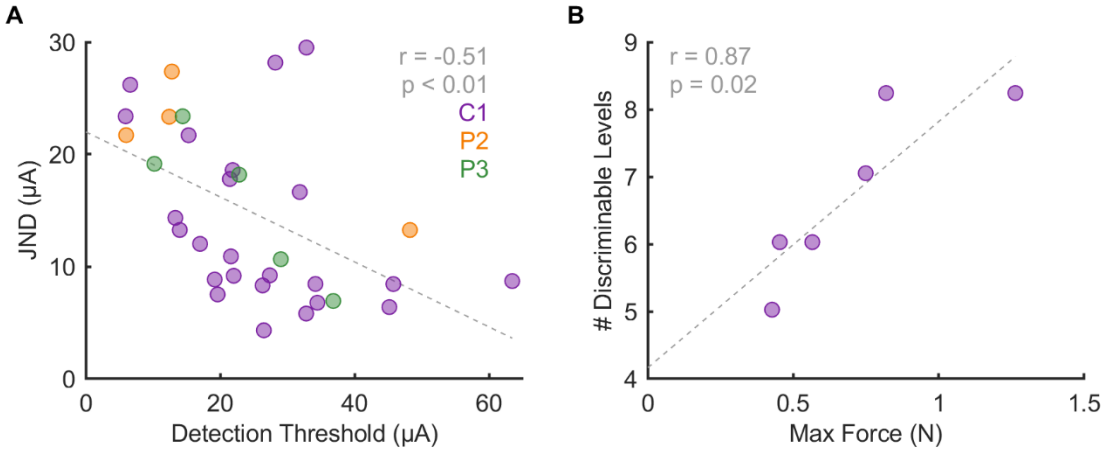

Supplementary Figure 3. A| The discriminability of an electrode (JND) is inversely correlated with its detection threshold. **B|** Electrodes that had a broader dynamic range (i.e., a greater maximum equivalent force) tended to yield more discriminable levels.

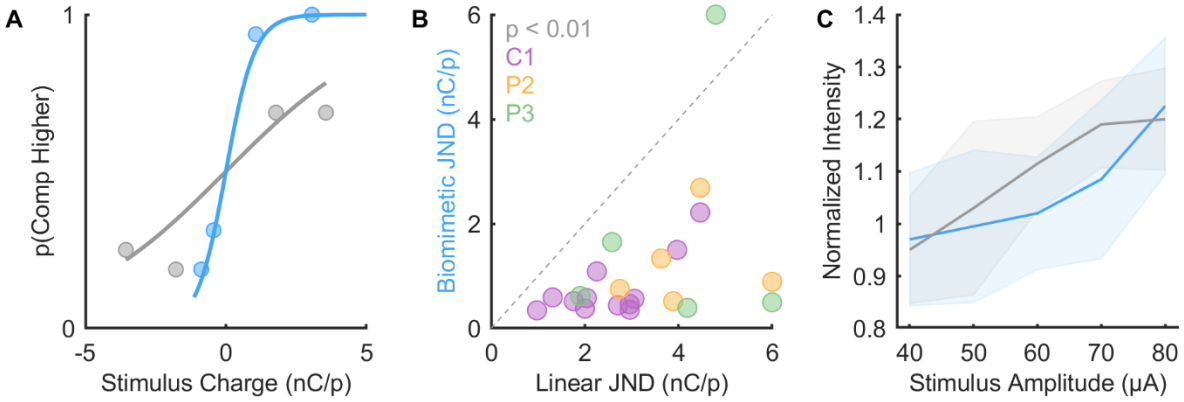

Supplementary Figure 4. Discrimination performance expressed in terms of injected charge. A| Psychometric functions for biomimetic and linear trains as a function of the difference in mean charge per phase between the standard and comparison, for one electrode. **B|** JNDs for biomimetic and linear stimuli across participants and electrodes (n = 20). Biomimetic stimuli yield significantly lower JNDs, expressed in terms of charge per phase (Wilcoxon signed-rank test, Z = 3.9, $p < 0.01$). **C|** Normalized intensity ratings for one channel. Linear ICMS does not give rise to significantly more intense sensations than does biomimetic ICMS when comparing stimuli with the same maximum amplitude. The mean relative intensity of the biomimetic stimuli was 92 ± 3% of the intensity of the linear ones (n = 5 electrode).

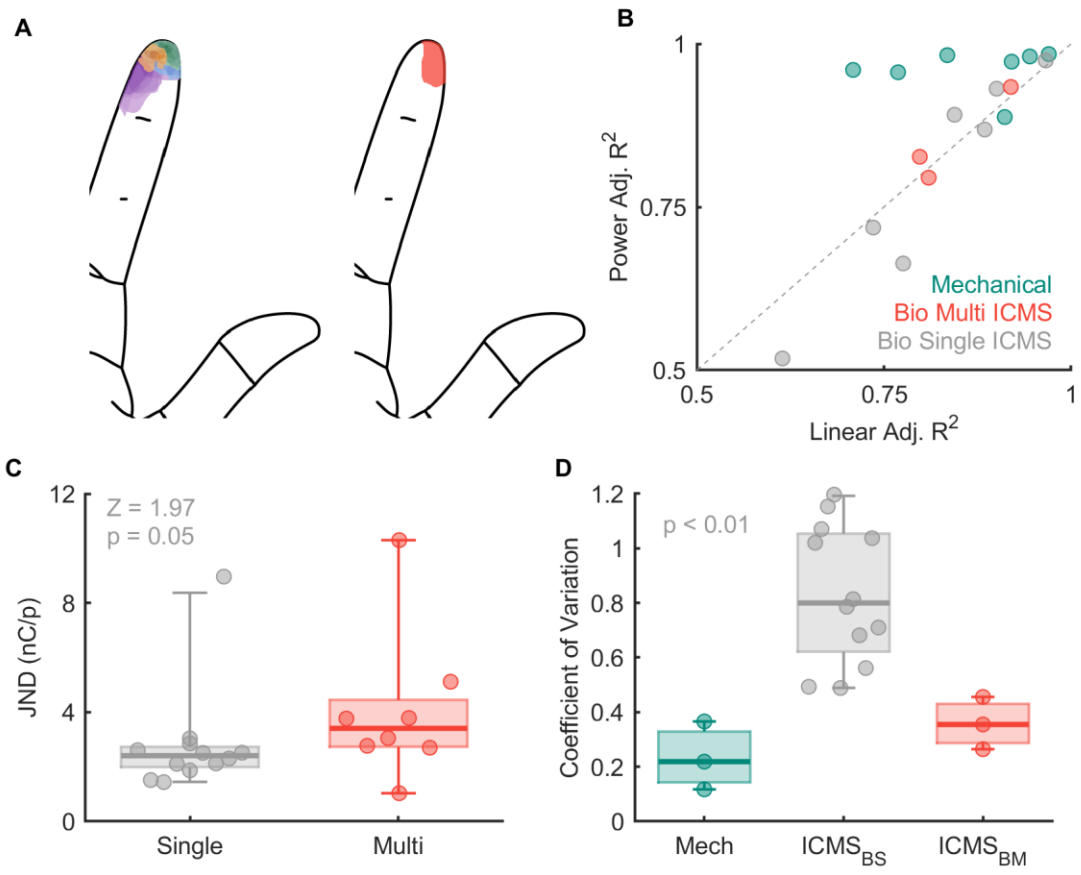

Supplementary Figure 5. A| Projected field locations for individual electrodes individually (left) and simultaneously (right) in one quad from participant C1. **B|** Linear fits are equivalent to power law fits for multi-channel stimulation. **C|** Discrimination performance for single or multi-channel biomimetic stimulation when expressed as charge per phase. **D|** Variability of responses is lower for multi-channel stimulation than for single-channel stimulation.

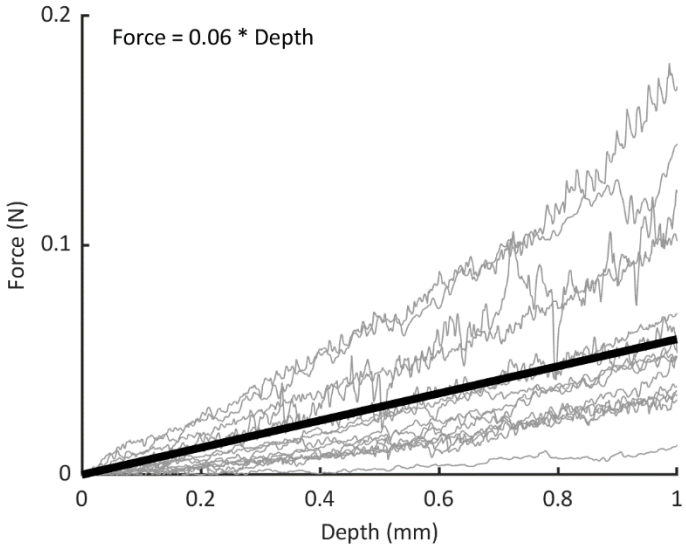

Supplementary Figure 6. Indentation depth vs force for 15 human participants using a 2-mm diameter tip with a universal testing machine (Instron). Each line denotes data from one participant, thick black line denotes the mean